

# New Polymeric Composites Based on Poly( $\epsilon$ -caprolactone) and Layered Double Hydroxides Containing Antimicrobial Species

Umberto Costantino,<sup>\*,†</sup> Valeria Bugatti,<sup>‡</sup> Giuliana Gorrasi,<sup>‡</sup> Francesca Montanari,<sup>†</sup> Morena Nocchetti,<sup>†</sup> Loredana Tammaro,<sup>‡</sup> and Vittoria Vittoria<sup>‡</sup>

CEMIN, Department of Chemistry, and INSTM, University of Perugia, Via Elce di Sotto 8, 06123 Perugia (PG), Italy, and Department of Chemical and Food Engineering and INSTM, University of Salerno, Via Ponte Don Melillo 1, 84084 Fisciano (SA), Italy

**ABSTRACT** Benzoate (Bz), 2,4-dichlorobenzoate (BzDC), and *p*- and *o*-hydroxybenzoate (*p*- and *o*-BzOH) anions with antimicrobial activity have been intercalated into  $[\text{Zn}_{0.65}\text{Al}_{0.35}(\text{OH})_2](\text{NO}_3)_{0.35} \cdot 0.6\text{H}_2\text{O}$ , layered double hydroxide (LDH), via anion-exchange reactions. The composition of the obtained intercalation compounds, determined by chemical, thermogravimetric, and ion chromatographic analyses, indicates that benzoate and benzoate derivative anions replace the nitrate counteranions, almost completely. Information on the interactions of the intercalated anions with the inorganic layer have been obtained from Fourier transform IR absorption spectroscopy and powder X-ray diffraction of the samples. It has been found that both the nature and the position of the aromatic ring substituents affect the value of the basal distance and the host–guest hydrogen bond network. Knowledge of the chemical composition, basal distance, and van der Waals dimensions of the guests has finally allowed the proposal of structural models of the intercalation compounds that have been used as fillers of poly(caprolactone), a biodegradable polymer. Films of polymeric composites were obtained by hot-pressing the powders of polymer and filler previously milled by a high-energy ball milling procedure. X-ray diffraction analysis and optical and scanning electron microscopy of the composites indicate that the LDH samples containing BzDC anions are delaminated into the polymeric matrix, whereas those containing *p*-BzOH anions maintain for the most part the crystal packing and give rise to microcomposites. Intermediate behavior was found for LDH modified with Bz and *o*-BzOH anions because exfoliated and partly intercalated composites were obtained. Preliminary antimicrobial tests indicate that the composites are able to inhibit the *Saccharomyces cerevisiae* growth of 40% in comparison with the growth in a pure culture medium. The composites can be studied as the model for “active packaging” systems because of the antimicrobial properties of the anions anchored to the LDH layer.

**KEYWORDS:** benzoate derivatives • layered double hydroxides • poly(caprolactone) • composites • antimicrobial activity

## INTRODUCTION

The preparation, characterization, and study of composites made up of polymeric matrixes and exfoliated layered crystals constitute one of the most promising research fields in material chemistry because the composites often possess enhanced mechanical, thermal, gas-barrier, and flame-retardant properties, when compared to those of the pristine polymer (1). Another important aspect of research on composites, not yet developed, regards the possibility of conferring to the polymeric material additional properties through the dispersion of nanofillers, constituted of an inorganic part that improves the mechanical and gas-barrier properties and of an organic moiety that brings functional groups capable of providing new properties. Nanofillers with such characteristics can be obtained by intercalation of functional molecular anions into inorganic layered hosts. For example, nanofillers obtained by exfoliation of a biocompatible layered double hydroxide (LDH)

intercalated with antiinflammatory drugs and dispersed into poly(caprolactone) (PCL) gave rise to polymeric composites in the form of fibers, films, or membranes with biomedical properties due to the slow release of the drug from the composite (2). It may be noted that, among lamellar solids, the LDHs constitute a very attractive class of hosts capable of producing inorganic–organic intercalation compounds because of their anion-exchange properties and the wide possibility of manipulation. These layered hosts, also known as “anionic clays” or “hydrotalcite-like compounds”, have the general formula  $[\text{M}^{\text{II}}_{1-x}\text{M}^{\text{III}}_x(\text{OH})_2](\text{A}_{x/n}) \cdot m\text{H}_2\text{O}$  where  $\text{M}^{\text{II}}$  is a divalent cation such as Mg, Ni, Zn, Cu, or Co and  $\text{M}^{\text{III}}$  is a trivalent cation such as Al, Cr, Fe, or Ga with  $\text{A}^{n-}$  an anion of charge  $n$ . The  $x$  value generally ranges between 0.2 and 0.4 and determines the positive-layer charge density and the anion-exchange capacity (3). The interlayer anions can be exchanged by other inorganic, organic, or metalloorganic anions and even by biomolecules (4) containing ionizable acidic groups to obtain novel materials of interest in the fields of photophysics and photochemistry (5), electrochemistry (6), catalysis (7), drug storage and release (8), pharmaceutical care (9), and environmental protection (10). Moreover, the obtained intercalation compounds can be used to prepare polymeric composites having the peculiar properties

\* Author to whom correspondence should be addressed. E-mail: ucost@unipp.it. Phone: +39.0755855565. Fax: +39.0755855566.

Received for review November 26, 2008 and accepted January 23, 2009

<sup>†</sup> University of Perugia.

<sup>‡</sup> University of Salerno.

DOI: 10.1021/am8001988

© 2009 American Chemical Society

of the filler. The new trend of the research is based on the fact that the active molecular anions, fixed by ionic bonds to the inorganic layer, not only can improve the compatibility with the polymer matrix (11) but also can be released with controlled kinetics in particular environments (2, 8). In this context, a research program has been undertaken to prepare suitable fillers of biodegradable polymers to obtain composites for “active packaging” systems. The present paper reports the preparation and characterization of model systems, formed by LDH intercalated with benzoate (Bz) and benzoate derivatives [2,4-dichlorobenzoate (BzDC), *p*-hydroxybenzoate (*p*-BzOH) and *o*-hydroxybenzoate (*o*-BzOH)] having antimicrobial properties and dispersed into PCL, a biodegradable polymer. The benzoate and benzoate derivatives are used as food preservatives and show toxicity at very high levels (maximum acceptable daily intake 5 mg/kg of body weight) (12). The study of the structural properties of composites at different percentages of intercalation compounds in PCL was performed, and these properties were correlated to the size, shape, and structural formula of the intercalated organic anions. The prepared composites are promising active food packaging systems because of the presence of antimicrobial agents that can control undesirable growth of microorganisms on the surface of foods.

## EXPERIMENTAL SECTION

**Materials.** Poly( $\epsilon$ -caprolactone) (CAPA 6501, average molecular weight 50 kDa) was purchased from Solvay (Italy). Sodium benzoate, sodium *o*-hydroxybenzoate, and 2,4-dichlorobenzoic acid and *p*-hydroxybenzoic acids were purchased from Sigma-Aldrich.

For the antimicrobial test, M.R.S. broth (de Man, Rogosa, Sharpe) of *Saccharomyces cerevisiae* was used on the M.R.S. agar (20 g/dm<sup>3</sup>).

**Preparation of ZnAl-LDHs.** LDH of the formula [Zn<sub>0.65</sub>Al<sub>0.35</sub>(OH)<sub>2</sub>](CO<sub>3</sub>)<sub>0.175</sub> · 0.5H<sub>2</sub>O was prepared according to the urea method (13). The corresponding chloride form, [Zn<sub>0.65</sub>Al<sub>0.35</sub>(OH)<sub>2</sub>](Cl)<sub>0.35</sub> · 0.6H<sub>2</sub>O, was obtained by titrating, at room temperature (rt), the carbonate form, dispersed in a 0.1 mol/dm<sup>3</sup> NaCl solution (1 g/50 cm<sup>3</sup>), with 0.1 mol/dm<sup>3</sup> HCl by means of a Radiometer automatic titrator operating at pH stat mode and with a pH value of 5. In order to obtain the nitrate form, ZnAl-LDH in chloride form was suspended in a CO<sub>2</sub>-free aqueous solution of 0.5 mol/dm<sup>3</sup> NaNO<sub>3</sub> (1 g/50 cm<sup>3</sup> of solution) and gently stirred for 24 h at rt. The recovered solid was washed three times with CO<sub>2</sub>-free deionized water and finally dried at rt over a saturated NaCl solution (75 % of relative humidity, RH). It has the formula [Zn<sub>0.65</sub>Al<sub>0.35</sub>(OH)<sub>2</sub>](NO<sub>3</sub>)<sub>0.35</sub> · 0.6H<sub>2</sub>O (ZnAl-NO<sub>3</sub>) and an anion-exchange capacity (IEC) equal to 2.95 mequiv/g. In the following, the intercalation compounds will be indicated as ZnAl-anion.

**Preparation of ZnAl-2,4-dichlorobenzoate (ZnAl-BzDC) and ZnAl-*p*-hydroxybenzoate (ZnAl-*p*-BzOH) Intercalation Compounds.** The intercalation of the benzoate derivatives (BzDC and *p*-BzOH) into ZnAl-LDH was obtained by equilibrating 1 g of ZnAl-NO<sub>3</sub> in 15 cm<sup>3</sup> of a 0.5 mol/dm<sup>3</sup> water/acetone (1/1, v/v) solution in the anions, previously prepared by titrating the corresponding acids with 1 mol/dm<sup>3</sup> NaOH until pH = 8. The suspensions were stirred at rt for 3 days. The obtained intercalation compounds were washed with CO<sub>2</sub>-free deionized water and dried at rt to 75 % RH.

**Preparation of ZnAl-benzoate (ZnAl-Bz) and ZnAl-*o*-hydroxybenzoate (ZnAl-*o*-BzOH) Intercalation Compounds.** The intercalation of benzoate and *o*-hydroxybenzoate anions was

achieved by equilibrating the nitrate form of LDH with a 0.5 mol/dm<sup>3</sup> aqueous solution of the anion (molar ratio organic anions/NO<sub>3</sub><sup>-</sup> = 3) for 24 h at rt. The recovered solids were washed three times with CO<sub>2</sub>-free deionized water and dried to 75 % RH.

**Films Preparation of PCL/LDH Organically Modified Composites.** The incorporation of the intercalation compounds into PCL was achieved by the high-energy ball milling (HEBM) method (11). Powders composed of PCL and of LDHs modified with the four organic anions (vacuum dried for 24 h) were milled in different percentages (w/w), at rt in a Retsch (Haan, Germany) centrifugal ball mill (model S100). The powders were milled in a cylindrical steel jar of 50 cm<sup>3</sup> with five steel balls of 10 mm of diameter. The rotation speed used was 580 rpm, and the milling time was 1 h.

The pure PCL, taken as the reference, was milled under the same experimental conditions as those of the composites. The milled powders were molded in a Carver laboratory press between two Teflon sheets, at 80 °C, followed by a quick quenching in an ice–water bath. Films of 100  $\mu$ m thickness were obtained and analyzed.

In the following, films obtained by milling will be coded as PCL/ZnAl-Bzn, PCL/ZnAl-BzDCn, PCL/ZnAl-*o*-BzOHn, and PCL/ZnAl-*p*-BzOHn, where *n* is the amount (worded as weight percentage) of ZnAl-Bz, ZnAl-BzDC, ZnAl-*o*-BzOH, and ZnAl-*p*-BzOH, respectively, present in the composites.

For comparison, a set of composites with the lowest content of corresponding intercalation compounds, obtained by grinding of the powders, was prepared and filmed, as previously described. Such last samples will be named as PCL/ZnAl-Bz3m, PCL/ZnAl-BzDC3m, PCL/ZnAl-*o*-BzOH4m, and PCL/ZnAl-*p*-BzOH4m.

**Analytical Procedures.** The Zn and Al contents of LDHs were obtained with standard ethylenediaminetetraacetic acid titration after having dissolved a weighed amount of the sample (~100 mg) in a few drops of concentrated HCl and diluting with water to 50 cm<sup>3</sup>.

The amount of NO<sub>3</sub><sup>-</sup> and organic counterions in solution was determined by ion chromatography using a Dionex 2000 ion chromatograph equipped with an ionic conductivity detector, after having equilibrated a given amount of sample (~100 mg) in 20 cm<sup>3</sup> of a 1 mol/dm<sup>3</sup> Na<sub>2</sub>CO<sub>3</sub> solution.

The amount of CO<sub>2</sub> evolved during the thermal treatment of ZnAl-Bz was determined by taking advantage of the reaction between CO<sub>2</sub> and Ba(OH)<sub>2</sub> with the formation of solid BaCO<sub>3</sub>. Weighed amounts (about 700 mg) of ZnAl-Bz were placed in a three-necked vessel and heated at a fixed temperature (150, 300, 350, and 400 °C) for 5 h in a vertical oven. A nitrogen flow was used as the carrier of the CO<sub>2</sub> evolved and sent up two gas bubblers, placed in series, each of them containing 150 cm<sup>3</sup> of an aqueous solution of 0.01 mol/dm<sup>3</sup> Ba(OH)<sub>2</sub>. After the indicated period (5 h), the concentration of the Ba(OH)<sub>2</sub> solutions was determined by titration with an aqueous solution of 0.01 mol/dm<sup>3</sup> HCl. The moles of CO<sub>2</sub> evolved were deduced as the difference between the initial and residual moles of Ba(OH)<sub>2</sub>.

**Antimicrobial Tests.** The antimicrobial tests were performed by using as microorganisms *S. cerevisiae*. The microbial population was assayed by counting colony-forming units (CFUs) using the pour-plate technique. Culture serially diluted was planted out on plates of M.R.S. agar and incubated at 32 °C for 2 days, and the CFU/cm<sup>3</sup> was measured over 2 days. In two plates, planted out with the same previous amounts of *S. cerevisiae* culture and containing 500  $\mu$ L of a physiological saline solution, films of pure PCL or PCL/ZnAl-*p*-BzOH10 (2 × 2 cm; 100  $\mu$ m thickness) were placed. The cultures were incubated at 32 °C, and the CFU/cm<sup>3</sup> was measured over 2 days. A plateau value of CFU/cm<sup>3</sup> was reached after 48 h. The antimicrobial film power was compared with that of a physiological saline solution

**Table 1. Acronyms of Molecular Ions Intercalated into ZnAl-LDH, Basal Distance, and Composition of the Intercalation Compounds**

anion	anion length (Å) <sup>a</sup>	<i>d</i> (Å) <sup>b</sup>	composition
Bz	5.98	15.5	[Zn <sub>0.65</sub> Al <sub>0.35</sub> (OH) <sub>2</sub> ]Bz <sub>0.35</sub> · 1H <sub>2</sub> O
<i>o</i> -BzOH	5.98	15.5	[Zn <sub>0.65</sub> Al <sub>0.35</sub> (OH) <sub>2</sub> ] <i>o</i> -BzOH <sub>0.27</sub> (NO <sub>3</sub> ) <sub>0.08</sub> · 1H <sub>2</sub> O
<i>p</i> -BzOH	6.57	15.3	[Zn <sub>0.65</sub> Al <sub>0.35</sub> (OH) <sub>2</sub> ] <i>p</i> -BzOH <sub>0.33</sub> (NO <sub>3</sub> ) <sub>0.02</sub> · 0.85H <sub>2</sub> O
BzDC	6.62	16.8	[Zn <sub>0.65</sub> Al <sub>0.35</sub> (OH) <sub>2</sub> ]BzDC <sub>0.32</sub> (NO <sub>3</sub> ) <sub>0.03</sub> · 1H <sub>2</sub> O

<sup>a</sup> Interatomic distance along the main axis of the anions calculated by the program *HyperChem* (14). <sup>b</sup> Basal spacing obtained from the second reflection of the PXRD.

containing the same amount of *p*-BzOH sodium salt as the sample analyzed (PCL/ZnAl-*p*-BzOH10).

**Instrumentation.** The powder X-ray diffraction (PXRD) patterns were taken, in reflection, with an automatic Bruker diffractometer, using nickel-filtered Cu K $\alpha$  radiation ( $\lambda = 1.54050$  Å) and operating at 40 kV and 40 mA, step scan 0.05° of 2 $\theta$ , and 3 s of counting time.

Fourier transform IR (FT-IR) absorption spectra were obtained by a Perkin-Elmer spectrometer, model Vertex 70 (average of 32 scans, at a resolution of 4 cm<sup>-1</sup>).

Thermal analysis (TGA/DTA) was carried out in an air atmosphere with a Mettler TC-10 thermobalance from rt to 1000 °C at a heating rate of 5 °C/min.

Information on the composite dispersion degree was obtained both with a Nikon inverted fluorescence optical microscope and with a Philips XL30 scanning electron microscope. Transparent films of about 80  $\mu$ m were prepared as described above, deposited on a glass holder, and analyzed with an optical microscope using an oil immersion objective 60 $\times$ . The scanning electron microscopy (SEM) micrographs of the samples metalized with gold were collected both on the surface and on the surface fracture of films performed in liquid nitrogen.

## RESULTS AND DISCUSSION

**Preparation and Characterization of Intercalation Compounds.** The intercalation compounds containing benzoate and benzoate derivatives have been prepared via ion-exchange reactions starting from ZnAl-NO<sub>3</sub> (see the Experimental Section). Table 1 reports the dimension (anion length) of the benzoate and benzoate derivatives, the basal distance, and the composition, deduced from chemical, ion chromatography, and TGA/DTA analyses, of the obtained intercalation compounds. It may be noted that the experimental conditions employed allow the molecular anions to replace almost completely the LDH nitrate counteranions.

The four samples display similar thermal behavior and, for the sake of brevity, only data relative to ZnAl-Bz are presented in Figure 1. The two endothermic weight losses, between 80 and 300 °C, are, very likely, related to the loss of 1 mol of co-intercalated water and 1 mol of water derived from dehydroxylation of the inorganic layers. The main weight loss between 300 and 500 °C may be ascribed to endothermic decarboxylation of benzoate and to exothermal combustion of the residual organic part. In order to confirm the occurrence of decarboxylation and discriminate between the endo and exo weight losses, the CO<sub>2</sub> evolved from the sample up to 400 °C was measured (see the Experimental Section). The inset of Figure 1 shows the percentage of CO<sub>2</sub>

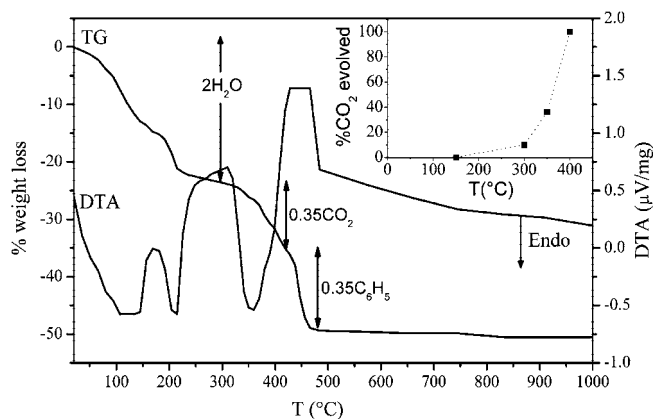


**FIGURE 1.** TGA and DTA curves of the sample ZnAl-Bz. Operative conditions: air flow; heating rate = 5 °C/min. Inset: CO<sub>2</sub> evolved upon Bz decarboxylation versus heating temperatures.

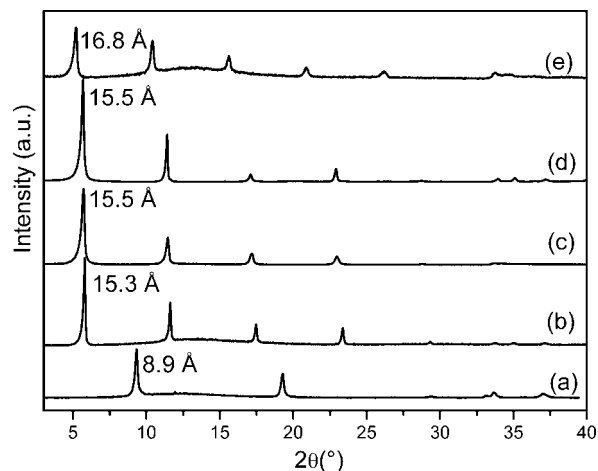


**FIGURE 2.** PXRD of the following intercalation compounds dried over a saturated NaCl solution (75% RH): (a) ZnAl-NO<sub>3</sub>; (b) ZnAl-*p*-BzOH; (c) ZnAl-*o*-BzOH, (d) ZnAl-Bz; (e) ZnAl-BzDC.

evolved with respect to the total calculated (0.35 mol per 1 mol of the intercalation compound) versus the sample decomposition temperature. It was found that at 300 °C the amount of CO<sub>2</sub> evolved was about 10% of the total and that it reached 100% at 400 °C. The data obtained are in good agreement with the TGA data also considering that the static conditions in which the experiments were conducted can anticipate the decarboxylation temperature with respect the TGA conditions. Finally, the PXRD patterns of the sample heated at 900 °C, shown in Figure S1 in the Supporting Information, indicate the formation of ZnO and ZnAl<sub>2</sub>O<sub>4</sub>. The TGA/DTA curves of the other intercalation compounds are reported in Figure S2 in the Supporting Information.

PXRD patterns of the intercalation compounds, in comparison with those of the pristine LDH, are shown in Figure 2. The samples are well crystallized in single phases having a basal distance increased in comparison with that of the nitrate form. The absence in the diffraction patterns of the intercalation compounds of the typical reflections of the nitrate form indicates that a solid solution of the residual nitrate phase into the benzoate phase has occurred (see Table 1).

FT-IR absorption spectroscopy of the ZnAl-Bz sample gave information on the interactions of intercalated ben-

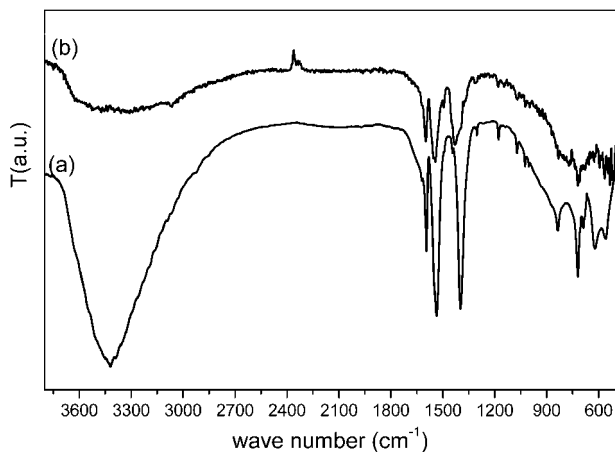


FIGURE 3. FT-IR spectra of ZnAl-Bz: (a) rt; (b) after heating at 300 °C for 5 h.

zoate anions and the brucite-type layer. Figure 3 shows the FT-IR spectra of the sample maintained at rt and of the sample previously heated at 300 °C. In the former case, the spectrum (Figure 3a) shows a strong broad band in the 3000–3750  $\text{cm}^{-1}$  range due to the stretching of the OH groups of the layer, involved in hydrogen bonds with hydration water molecules and carboxylate groups. The sharp and intense bands at 1537 and 1397  $\text{cm}^{-1}$  are ascribable to the asymmetric and symmetric stretching vibrations of the C–O bonds of  $\text{COO}^-$  groups. The in-plane skeletal vibration at 1595  $\text{cm}^{-1}$  and the two adsorption bands at 719 and 689  $\text{cm}^{-1}$ , due to the bending of the five adjacent hydrogen atoms of the ring, are typical signals of the monosubstituted aromatic ring. Moreover, the magnitude of the separation between of the carboxylate stretches [ $\Delta = \nu_{\text{as}}(\text{COO}^-) - \nu_{\text{s}}(\text{COO}^-)$ ] gives information on the mode of the carboxylate binding. In particular, the value of  $\Delta = 137 \text{ cm}^{-1}$  found is typical of sodium benzoate and suggests the presence of a monodentate carboxylate coordination (15). The FT-IR spectrum of the ZnAl-Bz, previously heated at 300 °C for 5 h (Figure 3b) does not have the broad band centered at 3420  $\text{cm}^{-1}$  because of the removal of hydration water and the condensation of OH groups of the layer, while the typical  $-\text{COO}^-$  stretching is still present. This observation, as established by TGA data, confirms that until 300 °C the endothermic processes are due to the elimination of the hydration and condensation of water and not to decarboxylation of the organic guest. A deeper analysis of the IR spectrum of the sample heated at 300 °C points out a shift of the  $\text{COO}^-$  group symmetric stretching toward higher wavenumbers and the calculated  $\Delta$  became 113  $\text{cm}^{-1}$ , indicating a chelating coordination of the carboxylate group.

The structural modification of ZnAl-Bz with temperature has also been studied by registration of the PXRD patterns in situ. Note that the first and second X-ray diffraction peaks of the sample heated up to 200 °C (see Figure 4) persist up to a temperature near 100 °C, even if they become broader from 50 °C. At temperatures higher than 150 °C, the sample becomes amorphous very likely because of the loss of co-intercalated water and starting dehydroxylation of the inorganic layer.

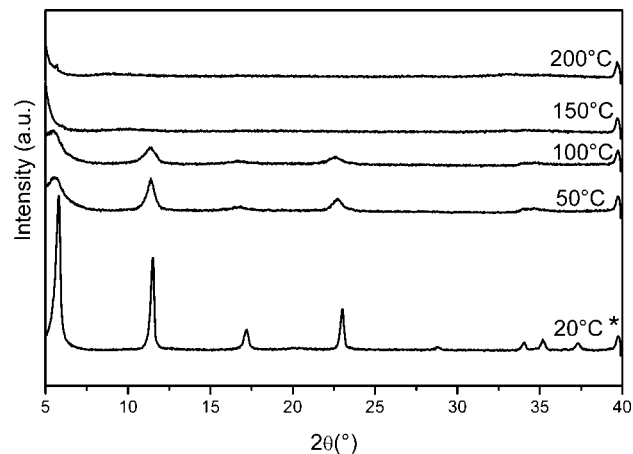


FIGURE 4. In situ high-temperature PXRD patterns of ZnAl-Bz at the indicated temperature: (\*) X-ray reflection of the aluminum sample holder.

Knowledge of the basal distance, and hence of the interlayer volume available to the guest species, of their number and anion dimension (see Table 1) allows a qualitative, but reliable, description of the arrangement of the guest species in the interlayer region. A structural model of the intercalation compounds is proposed, taking into account that the ion exchange is a topotactic reaction that occurs without appreciable modification of the structure of the layers that move apart from each other to make room for the guest species. The benzoate and benzoate derivative anion geometry has been optimized by applying a Hyperchem  $\text{MM}^+$  force field (14). A number of molecular anions equal to the positive fixed charges per unit area have been then positioned between the ZnAl-LDH layers. The  $\text{Ph}-\text{COO}^-$  bond of guests is almost perpendicular to the layer, and water molecules are located in planes adjacent to host layers together with  $\text{COO}^-$  groups. The model foresees the charge-balancing  $-\text{COO}^-$  groups lying alternately above and below the layer with the formation in the interlayer region of a monolayer of partially interdigitated species. The arrangement of benzoate anions in the interlayer region has been studied by several authors. Lagaly and co-workers in a wide study on the anion-exchange properties of MgAl-, ZnAl-, and ZnCr-LDH deduced an orientation of the benzene rings almost perpendicular to the layer plane (16). The same orientation of the guests was found by Jones and co-workers in the MgAl-benzoate, with a Mg/Al molar ratio of 2, obtained by a direct synthesis procedure (17). Finally, Capkova et al. (18) confirmed the proposed arrangement of guest molecules by molecular modeling.

Note that the nature and position of aromatic ring substituents affect the basal distance, as discussed by Forano et al. on similar systems (19). LDHs containing ortho-substituted benzoate derivatives (ZnAl-*o*-BzOH) have a basal distance equal to that of ZnAl-Bz because the long axis of the guest anions is unvaried (5.98 Å). On the other hand, when the guest is a para-substituted benzoate derivative, such as that in ZnAl-BzDC, the basal distance increased up to 16.8 Å according to the increased dimensions of the BzDC long axis (6.62 Å). However, the nature of the para substitu-

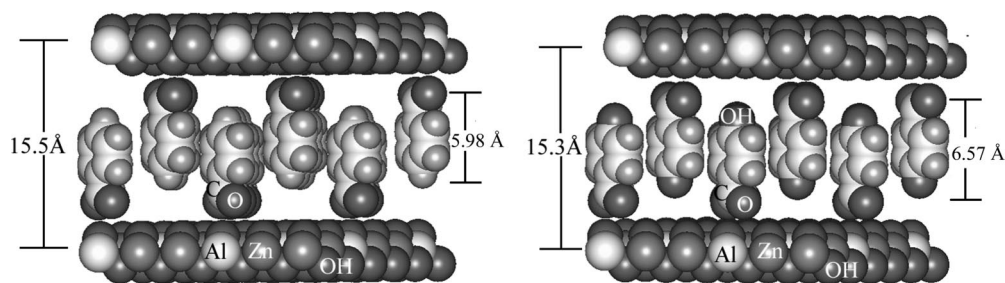


FIGURE 5. Computer-generated models showing the most probable arrangement of (left) Bz and (right) *p*-BzOH anions between the LDH layers.

ent should be considered as well. Indeed, the basal distance of ZnAl-*p*-BzOH is smaller (15.3 Å) than that of ZnAl-Bz even if the *p*-BzOH anion is 0.59 Å longer than Bz anion. Very likely the network of hydrogen bonds between the OH group of the guest and the OH group of the sheet through the hydration water brings the layer nearer. The distance between the oxygen atoms of the guest and the host involved in the hydrogen bond, through the co-intercalated water, evaluated on the basis of the proposed model is 4.4 Å. This value is very close to the calculated one on the basis of the sequence of hydrogen bonds (20). The structural models of intercalated Bz and *p*-BzOH are reported in Figure 5, while those of BzDC and *o*-BzOH are given in Figure S3 in the Supporting Information.

**Preparation and Characterization of PCL/Intercalation Compound Composite Films.** Different amounts of prepared intercalation compounds (ZnAl-Bz, ZnAl-BzDC, ZnAl-*o*-BzOH, and ZnAl-*p*-BzOH) have been incorporated into PCL by the HEBM technique (or by mechanical mixing). Films, about 100 μm in thickness, have been obtained by molding the powders in a laboratory press between two Teflon sheets (see the Experimental Section). The films, observed under an optical microscope, appear to be homogeneous, white, and opaque, without visible clusters of inorganic material. In comparison, films obtained from mechanically mixed powders appear to be inhomogeneous with visible clusters. The composite films have been characterized by means of X-ray diffraction, thermal analysis, FT-IR, optical microscopy, and SEM.

The X-ray diffraction patterns give information about the dispersion degree of the intercalation compounds into a PCL polymeric matrix. Figure 6 shows, in the  $2\theta = 2\text{--}40^\circ$  interval, the X-ray diffraction patterns of all intercalation compounds and composites obtained by the HEBM technique.

The PXRD patterns of composites containing ZnAl-*p*-BzOH in different weight percentages (Figure 6D) show, besides the typical reflections of crystalline PCL at  $2\theta = 21.3^\circ$  and  $23.9^\circ$  (labeled in the figure with an asterisk), the reflections of the unchanged intercalation compound. The presence of sharp and intense peaks relative to the pristine LDH indicates that the inorganic layer neither exfoliated nor intercalated the polymer, giving rise to microcomposites. A different behavior has been found for the other composites. The PXRD patterns of composites containing ZnAl-Bz and ZnAl-*o*-BzOH in different weight percentages (Figure 6A,C) show at  $2\theta = 4.55^\circ$  and  $4.7^\circ$ , respectively, a broad peak

ascribable to the inorganic–organic filler. A comparison with the PXRD pattern of the intercalation compound highlights a shift of the basal reflection toward lower values of  $2\theta$ , indicating that LDH is capable of partially intercalating PCL chains. In particular, composites containing ZnAl-Bz show an increase of the basal distance from 15.5 to 19.4 Å, while for ZnAl-*o*-BzOH, the observed increase is from 15.5 to 18.8 Å. Moreover, the low intensity and the broad shape of the peak is an indication of a partial exfoliation of the filler in the polymeric matrix, and the intensity of the basal reflection increases with an increase of the inorganic content in the polymer; it can also be attributed to the crystal size reduction by the HEBM process. PXRD patterns of composites containing ZnAl-BzDC (Figure 6B) have a trend similar to that discussed above even if the intensity of the basal peak of the intercalation compound is very low, especially for the composite loaded with 3% of inorganic filler.

To evaluate the meaning of the basal X-ray reflection intensity, a mechanical mixture of PCL powder with 3% of the intercalation compound ZnAl-BzDC (PCL/ZnAl-BzDC3m) has been prepared, and a comparison between the X-ray diffraction patterns of the milled sample and of the corresponding grinded mixture is presented in Figure 7. In the latter case, the simple grinding of the sample did not induce interactions of PCL with the intercalation compound and the basal X-ray reflection of the inorganic filler remained very intense and sharp, with the PXRD pattern being just a superposition of the two components' spectra.

The occurrence of the exfoliation of the inorganic filler into PCL can be deduced by evaluating the trend of the ratio between the intensity of the basal peak of the intercalation compound and the peak of PCL at  $2\theta = 21.3^\circ$  ( $R = I_{\text{basal peak}}/I_{\text{PCL} = 21.3^\circ}$ ) as a function of the inorganic content. Figure 8 reports the value of  $R$  versus the weight percentage of the LDHs modified with *p*-BzOH, *o*-BzOH, and Bz into composites.

It may be observed that  $R$  values can be fitted with a linear function having different slopes. In particular, for the composite PCL/ZnAl-*p*-BzOH, the  $R$  value doubles when the intercalation compound content doubles. Moreover, the  $R$  value of the same composite obtained by a mechanical mixture (PCL/ZnAl-*p*-BzOH4m) is close to that of PCL/ZnAl-*p*-BzOH4. These observations indicate that the exfoliation does not occur. In the other composites, the variation of  $R$  with the filler content is much lower, supporting the hypothesis that the fillers are not completely intercalated but a part

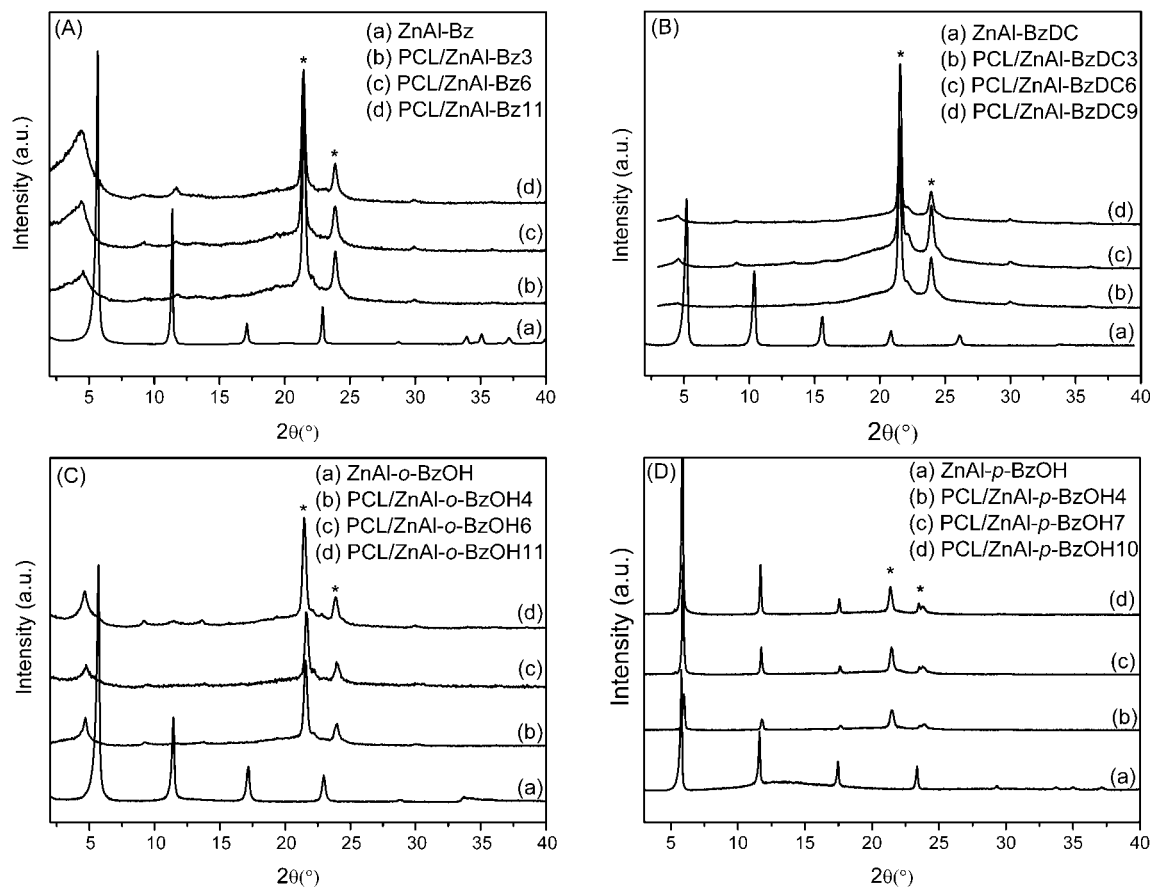


FIGURE 6. PXRD patterns of (A) ZnAl-Bz and composites; (B) ZnAl-BzDC and composites; (C) ZnAl-*o*-BzOH and composites; (D) ZnAl-*p*-BzOH and composites; (\*) X-ray reflection of crystalline PCL.

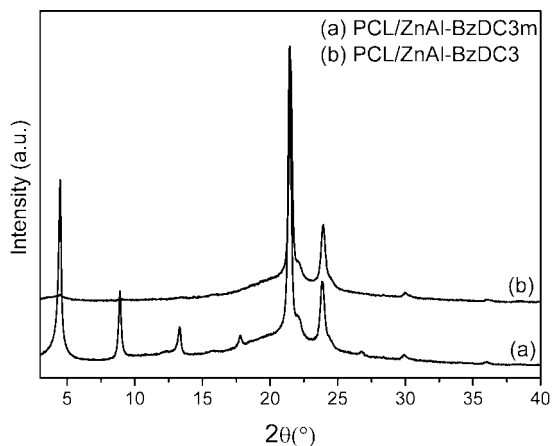


FIGURE 7. PXRD patterns of (a) PCL/ZnAl-BzDC3m and (b) PCL/ZnAl-BzDC3.

of the inorganic component is exfoliated, not contributing to the peak intensity.

The morphology and dispersion degree of the composite films have been investigated by optical microscopy and SEM. Parts A and B of Figure 9 show the micrographs obtained by optical microscopy of the PCL/ZnAl-BzDC6 and PCL/ZnAl-*p*-BzOH4 composites selected as representative samples of potential opposite situations: exfoliated and microcomposite. By optical microscopy, it is possible to evaluate the transparency of the films and then to get information about the dispersion degree. As expected, the PCL/ZnAl-BzDC6

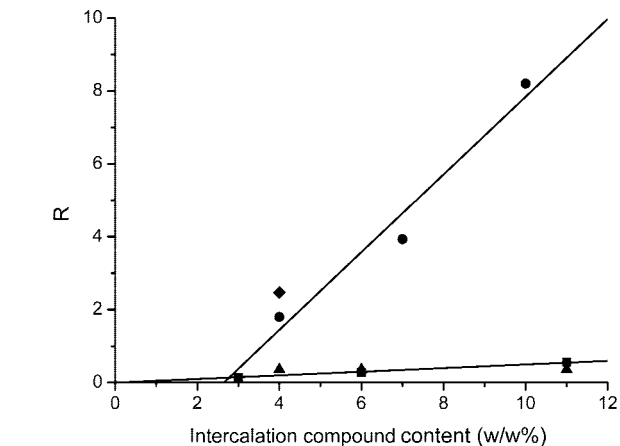


FIGURE 8. Ratio between the intensities of the basal peak of the intercalation compounds (from Figures 6 and 7) and the peak at  $2\theta = 21.3^\circ$  of PCL ( $R$ ) as a function of the intercalation compound content [PCL/ZnAl-*p*-BzOH composites (●); PCL/ZnAl-*p*-BzOH4m (◆); PCL/ZnAl-*o*-BzOH composites (▲); PCL-ZnAl-Bz composites (■)].

film (Figure 9A) is quite homogeneous, with the dark region probably due to the presence of packets of a few layers. Differently, the PCL/ZnAl-*p*-BzOH4 film (Figure 9B) presents an inhomogeneous texture with a gray background in which black and white regions are present, with the former ascribable to microcrystal aggregates and the latter to microvoids. The film surfaces of PCL/ZnAl-BzDC6 and PCL/ZnAl-*p*-BzOH4 were analyzed also by SEM and showed different features: a smooth surface in which rare inorganic particles are visible

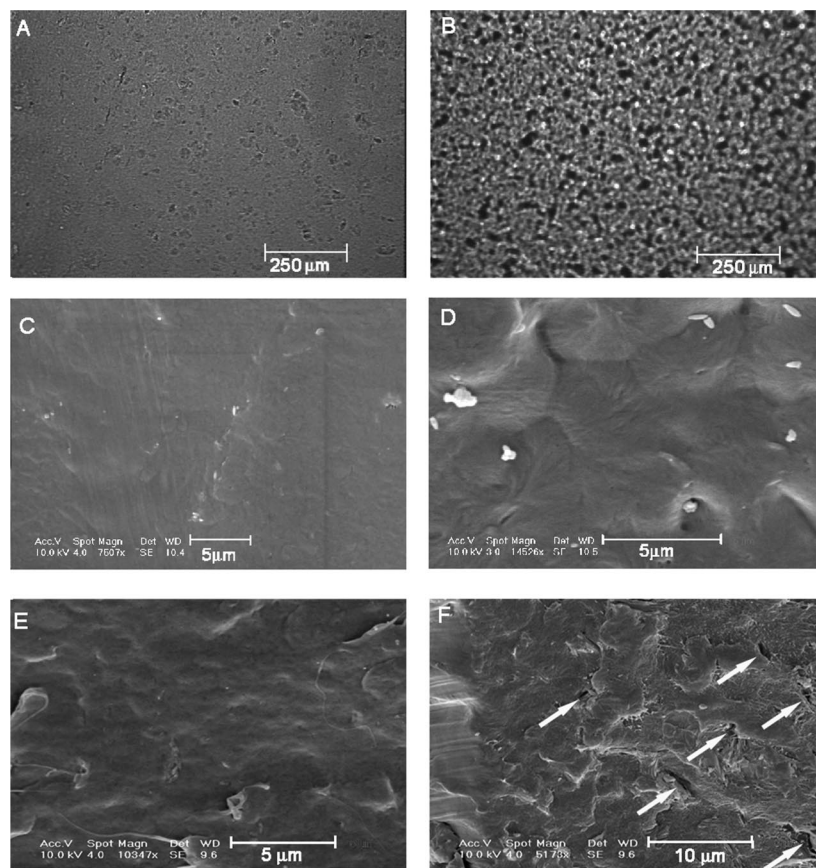


FIGURE 9. Optical micrographs of (A) PCL/ZnAl-BzDC6 and (B) PCL/ZnAl-*p*-BzOH4 films. SEM micrographs of (C) PCL/ZnAl-BzDC6 and (D) PCL/ZnAl-*p*-BzOH4 surface films and (E) PCL/ZnAl-BzDC6 and (F) PCL/ZnAl-*p*-BzOH4 surface fracture.

(Figure 9C) and a rough surface with evident inorganic particles (Figure 9D) and microvoids (observable in lower magnification, not shown). SEM micrographs of the PCL/ZnAl-BzDC6 and PCL/ZnAl-*p*-BzOH4 film surface fracture are reported in parts E and F of Figure 9, respectively. A composite film containing ZnAl-BzDC presents a very compact and uniform structure, indicating a good dispersion of the filler, while that containing ZnAl-*p*-BzOH is characterized by a steplike structure, a rough surface fracture with many crack initiations, indicated in Figure 9F with the arrows.

On the basis of the X-ray diffraction and of the microscopy data, it is possible to conclude that the interactions of guest–host and guest–guest that occur inside the interlayer region of the filler could affect the dispersion degree and the exfoliation of the intercalation compounds into the polymer. In the studied materials, the polymeric chains have to overcome the  $\pi$ – $\pi$  interactions among the aromatic rings of the intercalated anions to diffuse into the interlayer region. When the anion is *p*-BzOH, besides the  $\pi$ – $\pi$  interactions, a network of hydrogen bonds between OH groups of guest and OH groups of the opposite sheet, to form a pillared-like structure, hinders the intercalation of the polymer.

The content of the inorganic component (expressed as g of ZnO and ZnAl<sub>2</sub>O<sub>4</sub> per 100 g of composite) and the degradation temperature have been determined by recording the thermal decomposition of the composites up to 800 °C in air. For the sake of brevity, only TGA curves of the

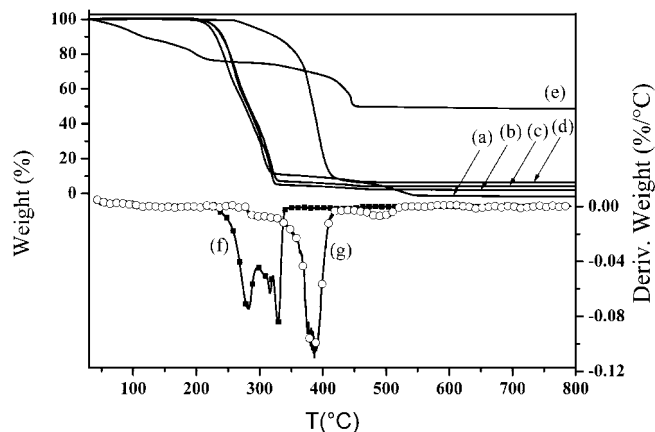


FIGURE 10. TGA curves of (a) PCL, (b) PCL/ZnAl-Bz3, (c) PCL/ZnAl-Bz6, (d) PCL/ZnAl-Bz11, and (e) ZnAl-Bz. Heating rate = 5 °C/min, in air flow. DTA curves of the composite PCL/ZnAl-Bz3 (f) and the pure PCL (g).

intercalation compound ZnAl-Bz and relative composites are shown in Figure 10, besides that of the pure PCL.

The TGA curve of PCL (Figure 10, curve a) displays one main degradation step with a midpoint value,  $T_d$ , of 383 °C, followed by a small tail at about 450 °C. The incorporation of the intercalation compound ZnAl-Bz within PCL anticipates the midpoint of thermal degradation, whose value slightly decreases with an increase in the ZnAl-Bz content. Similar results have been obtained for the other composites (see Figure S4 in the Supporting Information). Furthermore, it can be observed that the higher the interaction with the

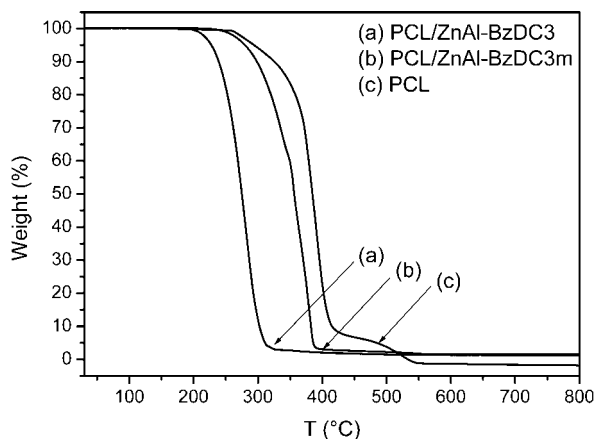


FIGURE 11. TGA measurements of (a) PCL/ZnAl-BzDC3, (b) PCL/ZnAl-BzDC3m, and (c) PCL. Heating rate = 5 °C/min, in air flow.

polymer, the more evident is the effect. This comes out of the analysis of Figure 11, where a comparison of the degradation curves for pure PCL, exfoliated PCL/ZnAl-BzDC3, and mechanical mixture PCL/ZnAl-BzDC3m is reported. The last sample shows a slightly lower degradation temperature, with respect to the pure polymer, whereas the effect in the exfoliated sample is much higher. It is not easy to justify such a behavior. The  $T_d$  midpoint of the composites is in the range where the intercalation compounds lose the constitution water (see Figure 1) with the formation of the oxides before decomposition of the organic guests. Hence, the anticipation of the  $T_d$  midpoint, relative to the pure PCL, could be ascribed to the action of the constitution water on the ester bonds giving rise to a base-catalyzed decomposition of the polymer. Similar results have been obtained in PCL composites containing fumed silica in which the hydroxyl groups present on the particle surface hydrolytically cleave the PCL's ester groups (21). Blends PCL/Nafion showed a reduction in the thermal stability in comparison with the pure PCL because PCL was hydrolyzed under heating in the presence of Nafion (22).

To have direct evidence of the thermal behavior of the composites in Figure 12, the degradation temperature of the pure PCL is compared with the dehydroxylation temperature of the intercalation compound and the degradation temperature of the composites with 3% of the dispersed intercalation compounds. In the exfoliated sample (PCL/ZnAl-BzDC3), the decrease of the degradation temperature is the most evident, being about 110 °C, whereas in PCL/ZnAl-*p*-BzOH3, it is only 58 °C.

All of the composites display similar behavior under FT-IR investigation, and for the sake of brevity, only data relative to ZnAl-Bz and respective composites will be discussed. Figure 13A shows the 1500–1650  $\text{cm}^{-1}$  region of FT-IR spectra of pure PCL, intercalation compound ZnAl-Bz, and composites with different loadings. Note that the asymmetric stretching of the  $\text{COO}^-$  group (1540  $\text{cm}^{-1}$ ) and the C=C stretching of the aromatic ring (1595  $\text{cm}^{-1}$ ) are present. It may also be observed that in this region there are no characteristic bands of pure PCL, and then it was attempted to correlate the absorbance at 1540  $\text{cm}^{-1}$  of the polymeric

composites with the filler loading. For this reason, it has been possible to determine in the composites both the presence and the amount of the intercalation compound with the carboxylate anion fixed on the inorganic layer.

The absorbance of the band at 1540  $\text{cm}^{-1}$  of the composites having the same thickness and corrected for the pure PCL FT-IR spectrum is plotted in Figure 13B as a function of the ZnAl-Bz content. A good linear dependence is evident, confirming the possibility of quantifying the intercalation compound content with a simple FT-IR analysis.

**Antimicrobial Properties of the Films.** Even though the antimicrobial properties of benzoate and benzoate derivatives have been known for a long time (23), it seemed of interest to carry out preliminary tests to prove that this property is still present in the polymeric composites.

The antimicrobial power of the PCL/ZnAl-*p*-BzOH10 film was then investigated by using the indirect viable cell counts, or plate counts, method, in which each colony that can be counted, called a CFU, is related to the number of viable bacteria in the sample. In this test, the yeast *S. cerevisiae*, planted on M.R.S. agar, was used as model bacteria. *S. cerevisiae* was selected because it is one of the most used yeasts in industrial/commercial food and beverage production and is even consumed as a nutritional supplement. Despite the large use in the above areas, various cases of fungemia caused by this yeast species in immune-deficient patients have been reported in recent years, suggesting that this species could be an opportunistic pathogen in such patients (24). *S. cerevisiae* shows functional and structural properties with *Candida albicans* (ALA1) that can cause systemic and mucosal infections (25). Moreover, *S. cerevisiae* has been described as being responsible for allergic bronchopulmonary fungal disease (26).

A PCL/ZnAl-*p*-BzOH10 film of dimensions 2 × 2 cm and thickness 100  $\mu\text{m}$  was deposited in a plate containing the *S. cerevisiae* culture together with 500  $\mu\text{L}$  of a physiological saline solution. To evaluate the effect of the polymer on the microbial growth, the previous procedure has been repeated using a pure PCL film. Moreover, in order to detect the antimicrobial activity of the pure *p*-BzOH anion, a physiological saline solution containing an amount of *p*-BzOH sodium salt equal to that of the sample analyzed (PCL/ZnAl-*p*-BzOH10) was added to a *S. cerevisiae* culture. Table 2 shows the bacterial growth of the yeast in the presence of pure PCL, a PCL/ZnAl-*p*-BzOH10 film, and the *p*-BzOH sodium salt solution compared with that of a pure culture medium. Similar results were obtained when *S. cerevisiae* was tested in stationary and logarithmic growth phases. Note that the polymer has no antimicrobial activity, with the *S. cerevisiae* concentration being very close to that of the yeasts in a pure culture medium (250 CFU/ $\text{cm}^3$ ). On the other hand, the presence of *p*-BzOH in the composite film inhibits the microbial growth by 40%, lowering the CFU/ $\text{cm}^3$  to 150. This value is comparable with that obtained with the pure *p*-BzOH sodium salt (140 CFU/ $\text{cm}^3$ ). These preliminary tests show that the antimicrobial power of *p*-BzOH is preserved in the



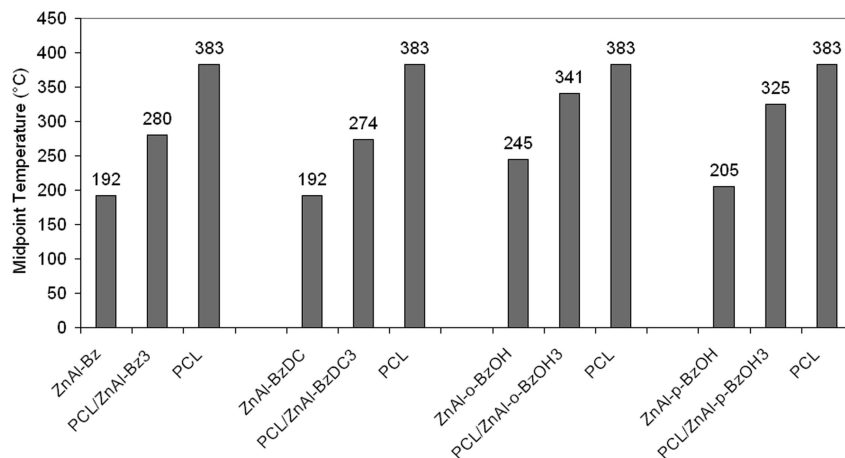


FIGURE 12. Comparison of the midpoint temperature (°C) derived from TGA analysis between PCL, intercalation compounds, and composites with 3% (w/w) of the intercalation compounds.

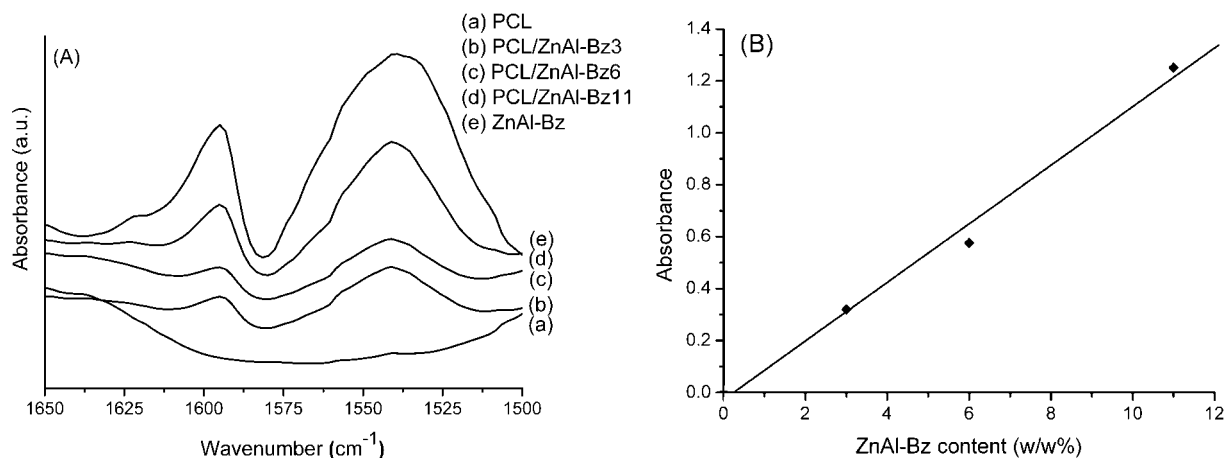


FIGURE 13. (A) IR spectra in absorbance of (a) PCL, (b) PCL/ZnAl-Bz3, (c) PCL/ZnAl-Bz6, (d) PCL/ZnAl-Bz11, and (e) ZnAl-Bz. (B) Relationship between the absorbance of the band at  $1540\text{ cm}^{-1}$  and the inorganic content of the intercalation compound ZnAl-Bz in the relative composites.

**Table 2. Comparison between the Microbial Concentration (CFU/cm<sup>3</sup>) of *S. cerevisiae* in the Culture Medium and in the Presence of the Indicated Samples<sup>a</sup>**

sample	CFU( <i>S. cerevisiae</i> )/cm <sup>3</sup>
pure culture medium	250 ± 8
PCL film	248 ± 10
<i>p</i> -BzOH sodium salt saline solution	140 ± 6
PCL/ZnAl- <i>p</i> -BzOH10 film	150 ± 8

<sup>a</sup> Growth conditions: 32 °C and 48 h.

polymeric composite, which may be considered a model for the development of active packaging systems.

## CONCLUSIONS

LDHs can be easily loaded with molecular anions having biological activity and the obtained intercalation compounds can be used as fillers of biodegradable polymers. When the filler exfoliates into the polymer, the guest anions not only improve the compatibility of the inorganic layer with the polymeric matrix, and hence the mechanical and barrier properties of the composite, but also confer to it their typical biological activity.

In the present case, ZnAl-LDH has been loaded with benzoate and benzoate derivatives with antimicrobial activity and the characterized intercalation compounds obtained have been dispersed into PCL. According to the nature of the guest, microcomposites and intercalated and/or exfoliated polymeric composites have been obtained and studied with different instrumental techniques. Both X-ray and IR analysis of films of composites gave a clear indication of the nature of the dispersion of the fillers and hence of their interactions with the polymer.

A preliminary antimicrobial test on yeasts for the PCL sample with 10% (w/w) of ZnAl-*p*-BzOH indicated deactivation of the microbial growth of 40%. Such a result gives evidence of the feasibility of the composites as “active packaging” materials.

**Acknowledgment.** This work was supported by a PRISMA 2005 project entitled “Biohybrids in polymeric matrices as controlled delivery of active molecules”. We thank Professor Giovanna Ferrari and Dr. Mariacarmela Bruno of the University of Salerno for their precious contribution to the antimicrobial test.

**Supporting Information Available:** PXRD of a ZnAl-Bz intercalation compound heated at 900 °C, TGA and DTA

curves of the ZnAl-*o*-BzOH, ZnAl-*p*-BzOH, and ZnAl-BzDC samples, computer-generated models showing the most probable arrangement of *o*-BzOH and BzDC anions between the LDH layers, and TGA curves of PCL/ZnAl-BzDC, PCL/ZnAl-*o*-BzOH, and PCL/ZnAl-*p*-BzOH composites at different contents of the intercalation compound. This material is available free of charge via the Internet at <http://pubs.acs.org>.

## REFERENCES AND NOTES

- (1) (a) *Polymer-clay nanocomposites*; Pinnavaia, T. J., Beall, G. W., Eds.; Wiley Series in Polymer Science; Wiley: New York, 2000. (b) Gorrasi, G.; Tortora, M.; Vittoria, V.; Pollet, E.; Lepoittevin, B.; Alexandre, M.; Dubois, P. *Polymer* **2003**, *44*, 2271. (c) *Polymer nanocomposites*; Mai, Y. W., Yu, Z. Z., Eds.; Woodhead Publishing Limited and RCR Press LCC: Cambridge, England, 2006. (d) Mangiacapra, P.; Raimondo, M.; Tammamo, L.; Vittoria, V.; Malinconico, M.; Laurienzo, P. *Biomacromolecules* **2007**, *8*, 775.
- (2) (a) Costantino, U.; Ambroggi, V.; Perioli, L.; Nocchetti, M. *Microporous Mesoporous Mater.* **2008**, *107*, 149. (b) Sammartino, G.; Marenzi, G.; Tammamo, L.; Bolognese, A.; Calignano, A.; Costantino, U.; Califano, L.; Tetè, S.; Vittoria, V. *Int. J. Immunopathol. Pharmacol.* **2006**, *19*, 53.
- (3) (a) Trifirò, F.; Vaccari, A. In *Solid-State Supramolecular Chemistry: Two and Three-dimensional Inorganic Networks, of Comprehensive supramolecular Chemistry*; Alberti, G., Bein, T., Volume Eds.; Pergamon and Elsevier Science Ltd. Press: Oxford, U.K., 1996; Vol. 7, p 251. (b) Jones, W.; Newman, S. P. *New J. Chem.* **1998**, 105. (c) *Layered Double Hydroxides: Present and Future*; Rives, V., Ed.; Nova Science Publishers: New York, 2001. (d) Khan, A. I.; O'Hare, D. J. *Mater. Chem.* **2002**, *12*, 1. (e) Leroux, F.; Taviot-Guého, C. *J. Mater. Chem.* **2005**, *15*, 3628.
- (4) (a) Choy, J. H.; Kwak, S. Y.; Jeong, Y. J.; Park, J. S. *Angew. Chem., Int. Ed.* **2000**, *39*, 4042. (b) Dsigaux, L.; Belkacem, M. B.; Richard, P.; Cellier, J.; Léone, P.; Cario, L.; Leroux, F.; Taviot-Gueho, C.; Pitard, B. *Nano Lett.* **2006**, *6*, 199. (c) Hwang, S. H.; Han, Y. S.; Choj, J. H. *Bull. Korea Chem. Soc.* **2001**, *22*, 1019.
- (5) (a) Ogawa, M.; Kuroda, K. *Chem. Rev.* **1995**, *95*, 399. (b) Latterini, L.; Nocchetti, M.; Costantino, U.; Aloisi, G. G.; Elisei, F. *Inorg. Chim. Acta* **2007**, *360*, 728.
- (6) (a) Han, E.; Shan, D.; Xue, H.; Cosnier, S. *Biomacromolecules* **2007**, *8*, 971. (b) Roto, R.; Villemure, G. *J. Electroanal. Chem.* **2007**, *601*, 112. (c) Mignani, A.; Luciano, G.; Lanteri, S.; Leardi, R.; Scavetta, E.; Tonelli, D. *Anal. Chim. Acta* **2007**, *599*, 36.
- (7) (a) Vaccari, A. *Appl. Clay Sci.* **1999**, *14*, 161. (b) Turco, M.; Bagnasco, G.; Costantino, U.; Marmottini, F.; Montanari, T.; Ramis, G.; Busca, G. *J. Catal.* **2004**, *228*, 43.
- (8) (a) Costantino, U.; Nocchetti, M. In *Layered Double Hydroxides and Their Intercalation Compounds in Photochemistry and Medicinal Chemistry*; Rives, V., Ed.; Nova Science Publishers: New York, 2001; Chapter 8. (b) Arco, M.; Gutiérrez, S.; Martin, C.; Rives, V.; Rocha, J. *J. Solid State Chem.* **2004**, *177*, 3954. (c) Dupin, J.; Martinez, H.; Guimon, C.; Dumitriu, E.; Fechete, I. *Appl. Clay Sci.* **2004**, *27*, 95. (d) Ambroggi, V.; Fardella, G.; Grandolini, G.; Nocchetti, M.; Perioli, L. *J. Pharm. Sci.* **2003**, *92*, 1407. (e) Ambroggi, V.; Fardella, G.; Grandolini, G.; Perioli, L.; Tiralti, M. C. *AAPS PharmSciTech* **2002**, *3*. (f) Ambroggi, V.; Fardella, G.; Grandolini, G.; Perioli, L. *Int. J. Pharm.* **2001**, *220*, 23. (g) Del Arco, M.; Fernández, A.; Martín, C.; Rives, V. *Appl. Clay Sci.* **2007**, *36*, 133. (h) Lu, Y.; Chen, S. C. *Adv. Drug Delivery Rev.* **2004**, *56*, 1621. (i) Tammamo, L.; Costantino, U.; Bolognese, A.; Sammartino, G.; Marenzi, G.; Malignano, A.; Tetè, S.; Mastrangelo, F.; Califano, L.; Vittoria, V. *Int. J. Antimicrob. Agents* **2007**, *29*, 417.
- (9) (a) Perioli, L.; Ambroggi, V.; Bertini, B.; Ricci, M.; Nocchetti, M.; Latterini, L.; Rossi, C. *Eur. J. Pharm. Biopharm.* **2006**, *62*, 185. (b) Perioli, L.; Ambroggi, V.; Rossi, C.; Latterini, L.; Nocchetti, M.; Costantino, U. *J. Phys. Chem. Solids* **2006**, *67*, 1079. (c) Rossi, C.; Schoubben, A.; Ricci, M.; Perioli, L.; Ambroggi, V.; Latterini, L.; Aloisi, G. G. *Int. J. Pharm.* **2005**, *295*, 47. (d) Perioli, L.; Nocchetti, M.; Ambroggi, V.; Latterini, L.; Rossi, C.; Costantino, U. *Microporous Mesoporous Mater.* **2008**, *107*, 180. (e) He, Q.; Yin, S.; Sato, T. *J. Phys. Chem. Solids* **2004**, *65*, 395. (f) Choi, S. J.; Oh, J. M.; Park, T.; Choy, J. H. *J. Nanosci. Nanotechnol.* **2007**, *7*, 4017. (g) Choi, S. J.; Oh, J. M.; Choy, J. H. *J. Mater. Chem.* **2008**, DOI: 10.1039/b711208d.
- (10) (a) Hussein, M.; Zainal, Z.; Yahaya, A.; Vui Foo, D. W. *J. Controlled Release* **2002**, *82*, 417. (b) Li, F.; Wang, Y.; Yang, Q.; Evans, D. G.; Forano, C.; Duan, X. *J. Hazard. Mater.* **2005**, *125*, 89. (c) Inacio, J.; Taviot-Gueho, C.; Forano, C.; Besse, J. P. *Appl. Clay Sci.* **2001**, *18*, 255. (d) Carretero, M. I.; Lagaly, G. *Appl. Clay Sci.* **2007**, *36* (Clays and Health Clays in Pharmacy, Cosmetics, Pelotherapy, and Environmental Protection Special Issue).
- (11) (a) Triantafyllidis, C. S.; LeBaron, P. C.; Pinnavaia, T. J. *J. Solid State Chem.* **2002**, *167*, 354. (b) Zanetti, M.; Lomakin, S.; Camino, G. *Macromol. Mater. Eng.* **2000**, *179*, 1. (c) Schadler, L. S. In *Nanocomposite Science and Technology*; Ajayan, P. M., Braun, P. V., Eds.; Wiley-VCH Verlag: Weinheim, Germany, 2003; Chapter 2. (d) Leroux, F.; Besse, J.-P. *Chem. Mater.* **2001**, *13*, 3507. (e) Tortora, M. R.; Gorrasi, G.; Sorrentino, A.; Vittoria, V.; Costantino, U.; Marmottini, F. *J. Polym. Sci., Part A: Polym. Chem.* **2005**, *43*, 2281. (f) Costantino, U.; Gallipoli, A.; Nocchetti, M.; Camino, G.; Bellucci, F.; Frache, A. *Polym. Degrad. Stab.* **2005**, *90*, 586. (g) Costantino, U.; Montanari, F.; Nocchetti, M.; Canepa, F.; Frache, A. *J. Mater. Chem.* **2007**, *17*, 1079.
- (12) (a) Joint FAO/WHO Expert Committee on Food Additives. Evaluation of the toxicity of a number of antimicrobials and antioxidants. Geneva, Switzerland, June 5–12, 1961. (b) , Concise International Chemical Assessment Documents (CICADs). *Benzoic acid and sodium benzoate*; World Health Organization: Geneva, Switzerland, 2000; ISBN 924153026X.
- (13) Costantino, U.; Marmottini, F.; Nocchetti, M.; Vivani, R. *Eur. J. Inorg. Chem.* **1998**, 1439.
- (14) *HyperChem*, Release 6.01 for Windows; Molecular Modeling System, distributed by Hypercube, Inc., Ontario, Canada, 2000.
- (15) (a) Zelenák, V.; Vargová, Z.; Györyová, K. *Spectrochim. Acta, Part A* **2007**, *66*, 262. (b) Arizaga, G. G. C.; Mangrich, A. S.; Wypych, F. *J. Colloid Interface Sci.* **2008**, *320*, 238. (c) Arizaga, G. G. C.; Mangrich, A. S.; Gardolinski, J. E. F. C.; Wypych, F. *J. Colloid Interface Sci.* **2008**, *320*, 168.
- (16) Meyn, M.; Beneke, K.; Lagaly, G. *Inorg. Chem.* **1990**, *29*, 5201.
- (17) Kooli, F.; Chisem, I. C.; Vucelic, M.; Jones, W. *Chem. Mater.* **1996**, *8*, 1969.
- (18) Kovar, P.; Pospisil, M.; Nocchetti, M.; Capkova, P.; Melanoma, K. *J. Mol. Model.* **2007**, *13*, 937.
- (19) Prévot, V.; Forano, C.; Besse, J. P. *Appl. Clay Sci.* **2001**, *18*, 3.
- (20) Huheey, J. E. In *Inorganic Chemistry: Principles of Structure and Reactivity*; Harper & Row Publishers: New York, 1983.
- (21) Chrissafis, K.; Antoniadis, G.; Paraskevopoulos, K. M.; Vassilou, A.; Bikiaris, D. N. *Compos. Sci. Technol.* **2007**, *67*, 2165.
- (22) Navarro Cassu, S.; Aparecida Zoppi, R. M.; Felisberti, I. *J. Appl. Polym. Sci.* **2004**, *92*, 3701.
- (23) Russell, N. J.; Gould, G. W., Eds. *Food Preservatives*; Springer: Dordrecht, The Netherlands, 2003.
- (24) Lanos, R.; Fernandez-Espinar, M.; Querol, A. *Antonie van Leeuwenhoek* **2006**, *90*, 221.
- (25) Gaur, N. K.; Klotz, S. A.; Henderson, R. L. *Infect. Immun.* **1999**, *67*, 6040.
- (26) Ogawa, H.; Fujimura, M.; Tofuku, Y. *J. Asthma* **2004**, *41*, 223.

AM8001988